Langmuir

Article

pubs.acs.org/Langmuir

# Structure and Dynamics Studies of Concentrated Micrometer-Sized Colloidal Suspensions

Fan Zhang,*[,†,§] Andrew J. Allen,[†] Lyle E. Levine,[†] Jan Ilavsky,[‡] and Gabrielle G. Long[†,‡]

[†]Material Measurement Laboratory, National Institute of Standards and Technology, 100 Bureau Drive, Gaithersburg, Maryland 20899, United States

[‡]X-ray Science Division, Argonne National Laboratory, 9700 South Cass Avenue, Argonne, Illinois 60439, United States

[§]Department of Physics, Northern Illinois University, DeKalb, Illinois 60115, United States

Supporting Information

**ABSTRACT:** We present an experimental study of the structural and dynamical properties of concentrated suspensions of different sized polystyrene microspheres dispersed in glycerol for volume fraction concentrations between 10% and 20%. The static structure, probed with ultrasmall-angle X-ray scattering, shows a behavior very similar to that of hard spheres. The equilibrium dynamics is probed with ultrasmall-angle X-ray scattering–X-ray photon correlation spectroscopy, a new technique that overcomes the limits of visible light-scattering techniques imposed by multiple scattering and is suitable for studies of optically opaque materials containing micrometer-sized structures. We found that the intensity autocorrelation functions are better described by a stretched exponential function and microspheres in a concentrated suspension move collectively. We also found that the inverse of the effective diffusion coefficients displays a peak with respect to the scattering vector that resembles the peaks in the static structure factors, which indicates that a long-lived, low free-energy state exists. The relaxation time is approximately inversely related to scattering vector, a behavior consistent with models that describe the dynamics in terms of random, local structural arrangements in disordered media.

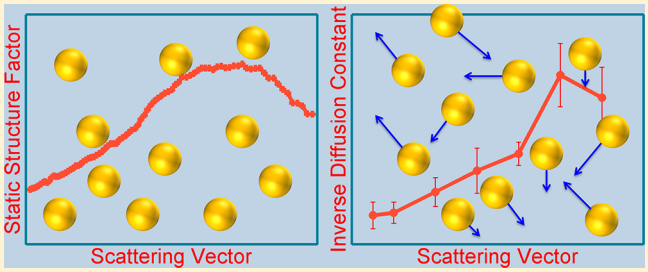


## INTRODUCTION

Colloidal suspensions of spherical particles in a liquid are among the simplest of complex fluids. Their understanding is seen as a stepping stone toward the goal of building a deeper knowledge of more complex soft matter systems, and is of both fundamental and practical importance. Fundamentally, studies of colloidal particles can lead to better understanding of structure and dynamics on the length and time scales relevant to individual particles. Practically, colloidal suspensions and their gels stand at the cross roads of material science, polymer science and engineering, and soft matter physics. Better understanding of such systems is likely to have a profound impact on the paint, adhesive, and cosmetics industries, for instance. While much effort, both theoretical and experimental, has been made to achieve this goal, a complete picture of the static structure and dynamics of colloidal dispersions has yet to emerge, largely due to a lack of experimental techniques for exploring the dynamic behavior of interacting particles.

Slow, complex relaxations in soft condensed matter materials have been successfully studied using coherent visible light-scattering techniques, most notably dynamic light scattering (DLS).[1] Prominent examples include studies of the dynamics of colloidal particles in suspensions or at surfaces. However, it has become apparent that there are limitations in the accessible length scale, and complications due to multiple scattering effects, both well-known obstacles intrinsic to the use of visible light. Coherent X-rays overcome both limitations and were naturally first used to revisit questions related to the dynamics and hydrodynamics of colloidal systems,[2−8] slow dynamics in polymers,[9−12] and capillary wave motions in complex fluids.[13−16] This extension of DLS is normally referred to as X-ray photon correlation spectroscopy (XPCS). XPCS, which was introduced less than two decades ago,[17−20] has greatly impacted many aspects of statistical physics and provided access to a wide range of physical events with slow equilibrium dynamics.

Conventional XPCS is based on a small-angle X-ray scattering (SAXS) pinhole-geometry configuration as realized at third-generation synchrotron radiation sources, where the undulator beams are partially coherent. The magnitude of the minimum accessible scattering vector, $q$, associated with this configuration, however, is limited by the beam stop that is used to block the intense main X-ray beam, and normally cannot reach $q < 0.001$ Å$^{-1}$. Here, $q = (4\pi/\lambda) \times \sin(\theta)$, with $\lambda$ being the wavelength and $2\theta$ the scattering angle. Inspection of the applicable $q$ ranges of DLS and XPCS shows a gap between about $1 \times 10^{-4}$ and $1 \times 10^{-3}$ Å$^{-1}$. A wide variety of microstructures in the size range from 1000 Å to several

**Received:** November 9, 2012
**Revised:** December 21, 2012
**Published:** January 7, 2013

   dx.doi.org/10.1021/la3044768 | Langmuir 2013, 29, 1379−1387

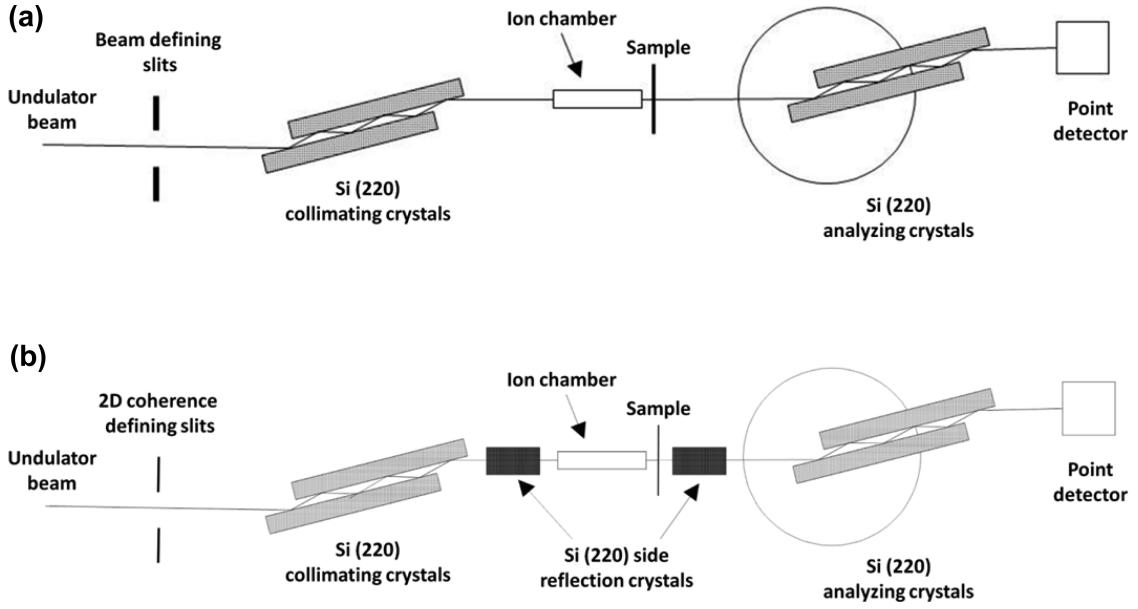


**Figure 1.** (a) Schematic of 1D USAXS configuration. (b) Schematic of USAXS−XPCS configuration, in which the addition of the Si (220) side reflection crystals provides point collimation, and the addition of 2D, 15 $\mu$m × 15 $\mu$m slits serves as a secondary coherent source.

micrometers[21,22] is best studied in this $q$ range because this is the regime where $qD \approx 1$, where $D$ is a representative dimension of the microstructure.

A few recent developments are aimed at overcoming this limitation. From the optical microscopy side, differential dynamic microscopy (DDM)[23−25] extends the effective low-$q$ limit by analyzing time series of microscope images with Fourier analysis. However, DDM is restricted to wide field imaging and can only probe the dynamics of dilute suspensions. Confocal differential dynamic microscopy,[26] on the other hand, can provide information on the dynamics of dense, opaque, fluorescent micrometer-sized objects, with fluorescence being a prerequisite, however. In the X-ray regime, near-field coherent X-ray imaging is also capable of revealing structural and dynamic information of materials,[27,28] albeit in a scattering $q$ range largely considered to be part of the range of DLS ($10^{-5}$−$10^{-4}$ Å$^{-1}$). Another technique, ultrasmall-angle X-ray scattering−X-ray photon correlation spectroscopy (USAXS−XPCS), was also developed[29,30] in response to this need. As compared to the above-mentioned techniques, USAXS−XPCS is a far-field scattering technique, which probes the particle dynamics directly in reciprocal space, and has the advantage of faster frequency response, should this be desired.

In this Article, we present both static and dynamic X-ray scattering measurements of the structure and dynamics of concentrated, charge-stabilized polystyrene microspheres dispersed in glycerol, a highly viscous fluid. The volume fractions range from 10% to 20%. Our goal is to elucidate the microspheres' motion in a viscous medium in the chosen volume and size range, and to present the USAXS−XPCS technique as a viable option for detailed investigations of colloidal dynamics in the previously inaccessible size range.

In the following sections, we first introduce the material systems and the experimental methods. We then present the methods used for the reduction and analysis of the static and dynamic data, followed by detailed results and discussion. Finally, we offer concluding remarks.

## EXPERIMENTAL METHODS

**Material System.** Monodisperse, aqueous colloidal suspensions of polystyrene (PS) microspheres with 10% solid mass fraction were acquired from Thermo Scientific Inc., Fremont, CA. (Certain trade names and company products are mentioned in the text or identified in illustrations to specify adequately the experimental procedure and equipment used. In no case does such identification imply recommendation or endorsement by National Institute of Standards and Technology, nor does it imply that the products are necessarily the best available for the purpose.) The mean, manufacturer-specified diameters of these microspheres were 1, 1.3, and 1.5 $\mu$m, respectively, with a stated size uniformity smaller than 3%. It is well-known that the time scales of colloidal dynamics are size dependent. Thus, suspensions with a narrow size distribution simplify the interpretation of the measured dynamics. The refractive index of the PS microspheres was 1.59 at an optical wavelength of 589 nm. Therefore, the as-acquired suspensions appear milky, making them nonideal samples for DLS measurements. The manufacturer-stated solid density of the PS microspheres was 1.05 g/cm$^3$.

PS, due to its X-ray scattering length density, has a small X-ray scattering contrast with water when in aqueous suspension. To increase the scattering contrast, each aqueous PS suspension was mixed with a predetermined amount of reagent-grade glycerol. The difference in scattering length density between glycerol and PS ($2.04 \times 10^{14}$ m$^{-2}$) is significantly greater than that between water and PS ($0.16 \times 10^{14}$ m$^{-2}$), which leads to a 160-fold increase in the X-ray contrast and scattering intensity. The water was removed by placing each mixture in a vacuum desiccation chamber for >600 h, although a small residual amount of water remained. Three samples with different concentrations of PS microspheres, (10, 15, 20)% by volume, were prepared for each particle size. A 15 s sonication was performed on the samples periodically as a precaution against particle aggregation. We found that these PS suspensions remained well dispersed throughout the sample preparation process, and before and after the X-ray scattering measurements. The final suspensions remained milky under visible light.

A second benefit of this transfer is that the viscosity of glycerol (1.5 Pa s at 25 °C) is about 3 orders of magnitude greater than that of water ($8.9 \times 10^{-4}$ Pa s at 25 °C). Thus, on transfer to glycerol, the dynamics of the suspensions are slowed considerably, enabling dynamic measurements to be made with an existing photodiode point detector at the beamline and reducing the required setup time


dx.doi.org/10.1021/la3044768 | Langmuir 2013, 29, 1379−1387

for the measurements. The best time resolution that this detector can achieve is ∼0.1 s.

**Ultrasmall-Angle X-ray Scattering Measurements.** The ultrasmall-angle X-ray scattering (USAXS) measurements were conducted at the USAXS beamline (32-ID, and later 15-ID) at the Advanced Photon Source (APS), Argonne National Laboratory.[31] This instrument employs Bonse−Hart-type double-crystal optics to extend the scattering vector $q$ range of small-angle X-ray scattering (SAXS) down to $10^{-4}$ Å$^{-1}$, which is normally inaccessible to pinhole SAXS cameras. We used collimated, monochromatic X-rays in the standard 1D collimated transmission geometry to measure the scattering intensity as a function of $q$. The instrumental configuration is illustrated in Figure 1a. The X-ray energy was 10.5 keV, which corresponds to an X-ray wavelength of 1.18 Å. USAXS measurements were performed in the $q$ range from $10^{-4}$ to 1 Å$^{-1}$ with a $q$ resolution of $\sim 1 \times 10^{-4}$ Å$^{-1}$. The beam size was 2.0 mm × 1.0 mm. The incident photon flux on the sample was $\sim 10^{13}$ photons per second. Data were collected at 600 points, logarithmically distributed throughout the $q$ range, and the data collection time for each data point was 1 s. A large dosage of hard X-ray radiation is known to create air bubbles in colloidal suspensions. To reduce the possibility of bubble formation, the sample position was scanned vertically in fixed steps during each USAXS scan. Radiation effects were then found to be minimal.

Each sample was loaded into a custom-made sample cell with polyamide-film entrance and exit windows and a 1 mm X-ray scattering path. To determine the instrumental scattering profile, two sets of USAXS measurements were collected: one with an empty cell, and the other with the cell filled with glycerol. The contributions of the polyamide windows and solvent to the scattering signal of each suspension were then removed in the data reduction process.

**Ultrasmall-Angle X-ray Scattering−X-ray Photon Correlation Spectroscopy Measurements.** XPCS applies the well-known principles of dynamic light scattering to coherent X-ray scattering. In general, a dynamic sample illuminated by partially coherent light gives rise to a time-varying speckle pattern. Utilizing the partially coherent X-rays generated by an undulator source, we used collimated, monochromatic X-rays in a 2D collimated transmission geometry to perform USAXS−XPCS measurements; the instrumental configuration is illustrated in Figure 1b. The coherence-defining slits were set at 15 $\mu$m × 15 $\mu$m, which gave the best beam coherence at the sample position. The X-ray energy was 10.5 keV. We used both a conventional top-up operating mode and a special reduced horizontal beam size operation mode of the APS storage ring, with the latter mode providing better coherence. We found that the operating modes of the storage ring affect the quality of the beam coherence, but not the observed sample dynamics.

The point-detection data collection mode of USAXS−XPCS[29] was used to acquire the XPCS data for the PS suspensions with equilibrium dynamics. With the photodiode point detector, we measured the intensity fluctuations at $q$ values of 0.00015, 0.0002, 0.0003, 0.0004, 0.0005, 0.0006, and 0.0007 Å$^{-1}$. We set the total data acquisition time to at least 20× the estimated dynamic time scale of the underlying equilibrium dynamics at each $q$, which was obtained with trial measurements. Depending on the individual dynamic time scale and the coherent scattering intensity, we chose the time resolution at 1 s or 500 ms, with a readout delay of ∼100 ms.

The time resolution of this experiment is limited by the photodiode detector. To further slow the dynamic time scale, we performed the USAXS−XPCS measurements at 5 °C, which effectively increases the viscosity of the solvent by a factor of ∼7.5 when compared to the viscosity at room temperature (25 °C). The temperature of the sample cell was controlled with a Linkam TH600 thermal stage (Linkam Scientific Instruments Ltd., Tadworth, UK), which uses both electrical resistive heating and liquid nitrogen circulation to provide rapid heating and cooling. The heating/cooling rate was set at 50 °C/min. We estimate that the temperature deviation from the thermocouple readout was less than 1 °C, and the temperature gradient in the sample was insignificant.

**USAXS Data Reduction and Analysis Methods.** The 1D collimated USAXS data reduction and analysis were performed using the standard SAXS data analysis package Irena,[32] developed at the APS. To eliminate the numerical error introduced by the desmearing process,[33] we performed data reduction and analysis on the slit-smeared data, which is done by convolving the absolute calibrated scattering intensity $I(q)$ with a rectangular slit. The width of the slit is determined by the chosen crystal optics; the length of the slit is related to the sample to detector distance and the size of the photodiode detector.

The reduced scattering intensity profiles $I(q)$ show a large number of Bessel oscillations that persist to the high-$q$ end of each data set. This attribute of the data indicates that the PS particles are spherical in geometry and have a very narrow size distribution. To extract the exact size distribution of the PS microspheres, we analyzed the scattering profile assuming the scattering form factor for spheres, and a consequent single sphere scattering intensity, $I_0(q)$, is given by:

$$I_0(q) = (\Delta\rho)^2 V^2 \left[ 3\frac{\sin(qr) - qr\cos(qr)}{(qr)^3} \right]^2 \quad (1)$$

where $\Delta\rho$ is the difference between the scattering length densities of the solute and solvent, and $r$ and $V$ are the radius and volume of the sphere, respectively. To avoid complications introduced by the unknown form of the scattering structure factor, the high-$q$ region of the scattering profile was modeled using a least-squares analysis method based on integrating eq 1 over a Gaussian volume size distribution. In this high-$q$ region, the particle interference can be regarded as negligible.

For a concentrated, isotropic system, the form factor and structure factor contributions to the scattering intensity are separable. In our case:

$$I(q) = \frac{\varphi}{V} I_0(q) S(q) \quad (2)$$

where $\varphi$ is the volume fraction of particles within the sample volume, and $S(q)$ is a structure-factor representation. In our analysis, the scattering structure factor was found by dividing the USAXS data by the size-averaged single particle scattering intensity, which was obtained by convolving the single particle scattering intensity with the particle size distribution.

**USAXS−XPCS Data Reduction and Analysis Methods.** XPCS probes the dynamic properties of matter by measuring the temporal correlation of the scattering intensity, which yields the characteristic relaxation times of the sample. Specifically, the intensity autocorrelation function is defined by:[34]

$$g_2(t) = \frac{\langle I(t + t')I(t')\rangle_E}{\langle I(t')\rangle_E^2} \quad (3)$$

where $I(t)$ is the integrated scattering intensity in an interval $\Delta t$ around a time $t$, and the angular brackets in eq 3 denote an ensemble average. This autocorrelation function can be related to the intermediate scattering function of the sample, following:

$$g_2(t) = 1 + \beta |f(q, t)|^2 \quad (4)$$

where $f(q, t) = S(q, t)/S(q)$ is the normalized intermediate scattering function. Here, $S(q) = S(q, 0)$ denotes the static structure factor and $S(q, t)$ is the structure factor at time $t$. $\beta$ is the optical contrast, which, under ideal experimental conditions (e.g., fully coherent radiation and no readout noise), would be equal to unity. In XPCS experiments, $\beta$ takes a lower value due to incoherent averaging introduced by the partially coherent X-ray beam, the geometrical configuration of the beamline, and readout noise. In our analysis, $I(t)$ was the photodiode readout (scattering intensity) normalized by the ion chamber readout (incident intensity). We have previously shown that this normalization does not affect the measured dynamics.[29]

The relaxation time represented by the calculated intensity autocorrelation function was further analyzed by modeling the autocorrelation function with a stretched exponential form (also known as the Kohlrausch−Williams−Watts (KWW) function[35]). It is defined as


dx.doi.org/10.1021/la3044768 | Langmuir 2013, 29, 1379−1387

$$g_2(t) = \beta \exp\left(-2 \times \left(\frac{t}{\tau}\right)^{\gamma}\right) + 1 \quad (5)$$

Here, $\tau$ is the characteristic relaxation time, and $\gamma$ is an exponent (the Kohlrausch exponent), which characterizes the shape of the autocorrelation function. In eq 5, $\gamma = 1$ represents the case of simple free diffusion as in Brownian motion, while $\gamma < 1$ commonly occurs for dynamics of glass-forming liquids near their glass transition points. It is with eq 5 that we extract the relaxation time constants of the particle diffusion in these concentrated PS suspensions.

## RESULTS AND DISCUSSION

The absolute-calibrated, differential-scattering cross sections from 1.0, 1.3, and 1.5 $\mu$m PS glycerol suspensions at 10%, 15%, and 20% vol are shown in Figure 2a, b, and c, respectively. At $q$ higher than $1 \times 10^{-3}$ Å$^{-1}$, the shape of the scattering profiles does not depend on the volume concentration and shows a large number of Bessel oscillations, characteristic of scattering from highly uniform spherical objects. We used a least-squares analysis method to analyze the Bessel oscillations at $q$ higher than $1 \times 10^{-3}$ Å$^{-1}$. The assumed Gaussian volume size distribution convolutes the scattering intensity of a single sphere, as specified in eq 1, and results in the final scattering intensity. The results from the 20% volume, 1.3 $\mu$m PS microspheres in glycerol sample are shown in Figure 3, in which the blue solid line shows the scattering from the size-averaged single particle scattering intensity, and the inset shows the Gaussian size distribution of the PS microspheres. We found that the size distribution can be described with mean diameter ≈1.319 $\mu$m and Gaussian width ≈0.047 $\mu$m, Å. Both of these parameters are close to the manufacturer-specified values and confirm that the PS microspheres indeed have a very narrow size distribution. In addition, we did not observe any upturn at the very low-$q$ range of the USAXS profiles, which indicates that the PS microspheres do not aggregate and remain well dispersed.

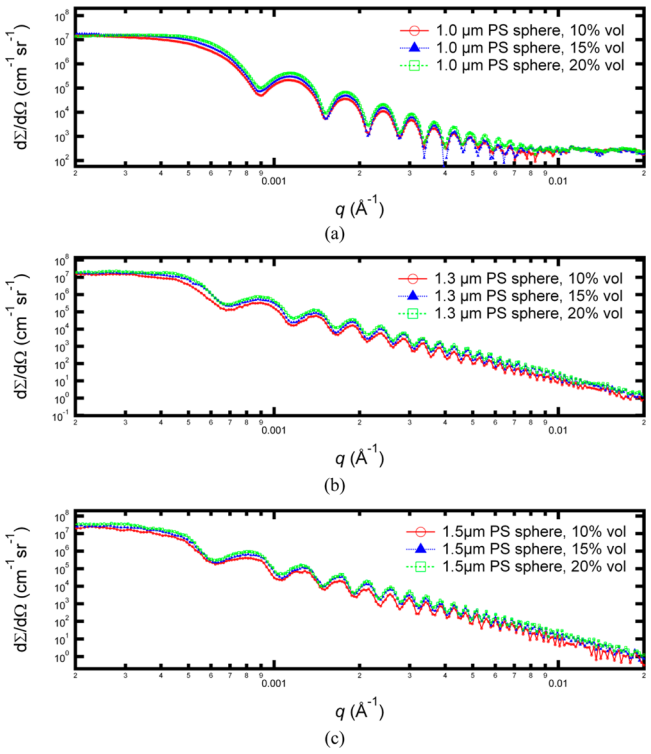


**Figure 2.** USAXS scattering profiles for (a) 1.0 $\mu$m PS spheres at 10%, 15%, and 20% vol concentrations; (b) 1.3 $\mu$m PS spheres at 10%, 15%, and 20% vol concentrations; and (c) 1.5 $\mu$m PS spheres at 10%, 15%, and 20% vol concentrations. [Uncertainties are smaller than the symbol sizes.]

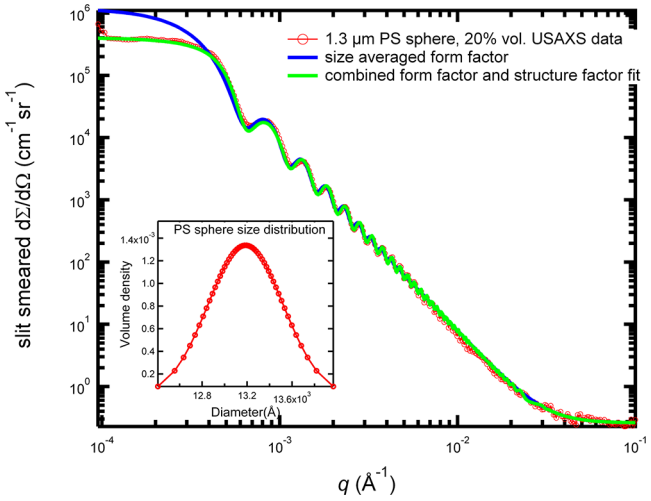


**Figure 3.** An example of USAXS analysis for the sample with 1.3 $\mu$m PS spheres at 20% vol. The size distribution, shown in the inset, is acquired from least-squares fitting of the region where $q$ is higher than $1 \times 10^{-3}$ Å$^{-1}$ of the USAXS profile. A structure factor was adopted to account for the intermicrosphere interference.

The size-averaged single particle scattering intensity describes the measured intensity well for the high-$q$ region. The low-$q$ region, however, shows significant deviations. This difference, as shown in Figure 3, is due to the fact that interparticle interactions exist in concentrated colloidal dispersions. In our system, glycerol is a polar solvent, and PS microspheres in glycerol form a typical colloidal dispersion. The interactions between the PS microspheres, which are charged particles, are best described by the Derjaguin–Landau–Verwey–Overbeek (DLVO) theory.[36] In the framework of DLVO theory, the long-range, attractive van der Waals interaction is balanced by a screened electrostatic repulsive interaction introduced by the charges at the surfaces of the colloids. In the case of PS suspensions, it has been shown that, at least from the structure factor point of view, the colloidal particles interacting via DLVO interactions can be reliably assumed to have effective hard-sphere interactions due to the fact that the length scale of the Debye layer is much smaller than the particle size.[3,4,37−39] Here, outside of the Debye layer, the charges on these particles are screened and the particles resembles neutral hard spheres.

We have performed structure factor analyses with both a hard-sphere potential and a Hayter–Penfold RMSA (rescaled mean spherical approximation) potential, which allows for inclusion of the interparticle interference effects due to screened Coulomb repulsion between charged particles in a dielectric medium.[40] We found that both potentials describe the structure factors and the measured intensity profiles well, with the Hayter–Penfold RMSA model fitting the data marginally better, possibly due to its larger number of fitting parameters.

The scattering structure factor was found by dividing the USAXS data by the size-averaged single particle scattering intensity, for example, the USAXS data and the single particle profile in Figure 3. Examples of the scattering structure factors are shown in Figure 4a. We observed that the magnitude of the


dx.doi.org/10.1021/la3044768 | Langmuir 2013, 29, 1379−1387

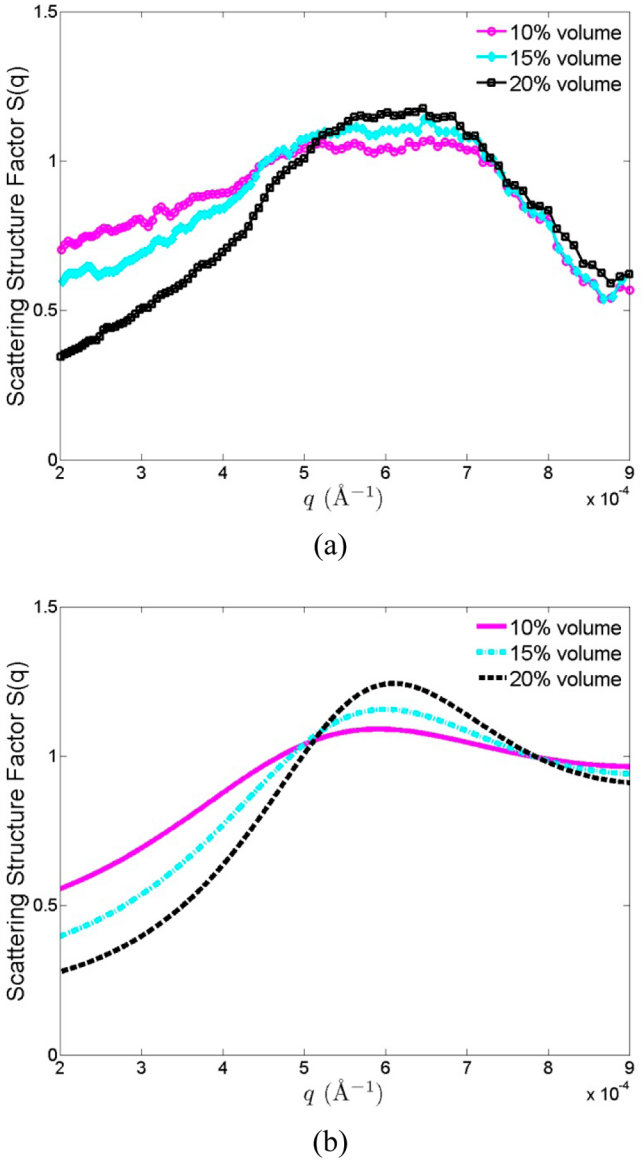


**Figure 4.** (a) Experimental structure factor for 10%, 15%, and 20% vol, 1.0 $\mu$m PS microspheres in glycerol. (b) Theoretical Percus–Yevick structure factor for 1 $\mu$m-diameter monodisperse hard spheres at 10%, 15%, and 20% vol.

pronounced peak in the scattering structure factor increases as the volume fraction of PS microspheres increases, corresponding to the increased interparticle interaction between the microspheres. The structure factor can be approximately described with the Percus–Yevick pair-distribution function,[41] which applies to monodisperse particles with a hard-sphere interaction potential. The theoretical Percus–Yevick structure factor functions corresponding to the samples in Figure 4a are plotted in Figure 4b. Evidently, this model provides a good description of the experimental structure factors at all volume fractions, and, in particular, accurately reproduces the height and position of the primary interference peak. Moreover, the decrease at the low-$q$ end of the experimental structure factor is well described by the model, which suggests that the osmotic compressibility of the PS microspheres agrees well with the hard-sphere equation of state.[36] We attribute the small difference between Figure 4a and b to the charged sulfate groups that are on the surface of the PS spheres, which inevitably modifies, albeit slightly, the interparticle interaction at a distance greater than the diameter of the PS microspheres. Our result is in good agreement with a previous SAXS study of PS suspensions in glycerol,[3] even though the nominal size of PS microspheres was much smaller (66 nm). The fact that the hard-sphere potential fits the scattering structure factor confirms that no significant aggregation of PS microspheres exists in the suspension, which agrees with independent Zeta potential results where their high absolute values directly lead to excellent stability and dispersibility of the microspheres.

In our USAXS–XPCS experiments, the observed dynamics reflect the motion of the PS microspheres in a medium of glycerol with a small amount of residual water that has some effect on the viscosity. Here, despite the remnant water, we assume that the medium is homogeneous because both glycerol and water are polar solvents and mix well with each other. We measured the intensity fluctuations of these simple PS microsphere suspensions at a series of $q$ values and calculated the intensity autocorrelation functions on the basis of the normalized coherent-scattering intensities from these measurements. Figure 5, as an example, shows the representative

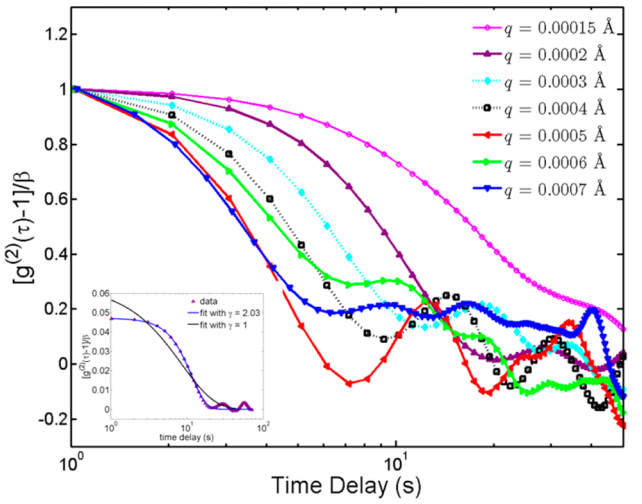


**Figure 5.** Examples of the intensity correlation function for the sample with 1.3 $\mu$m PS spheres at 20% vol. After acquisition of the fixed $q$ intensity fluctuation at $q$ = 0.00015, 0.0002, 0.0003, 0.0004, 0.0005, 0.0006, and 0.0007 Å$^{-1}$, respectively, eq 3 was used to calculate the corresponding intensity correlation functions shown in this figure. These correlation functions have been normalized by their respective optical contrast. The inset shows the fits of the intensity autocorrelation function at $q$ = 0.0002 Å$^{-1}$ with the simple exponential decay function ($\gamma$ = 1) and KWW function ($\gamma \neq 1$).

intensity autocorrelation functions with delay times from 1 to 50 s, obtained for 1.3 $\mu$m PS spheres at 20% volume fraction. These correlation functions have been normalized by their respective optical contrast $\beta$. Here, the optical contrast is $q$-dependent due to the different signal-to-noise level from the photodiode detector that was used in these measurements. We have previously shown that, although the scattering contrast is modified due to the existence of detector noise, the observed time scale is unaffected.[29]

From Figure 5, it is evident that faster dynamics are associated with larger scattering vector $q$, an expected phenomenon considering that the short-range, local fluctuations (large $q$) occur more rapidly than long-range fluctuations (small $q$) in interacting colloidal suspensions. Similar to Gutt et


dx.doi.org/10.1021/la3044768 | Langmuir 2013, 29, 1379–1387

al.,[42] we observed small fluctuations in the long time-delay end of the intensity autocorrelation functions due to the partially coherent nature of the beam and the limited detector resolution.

The intensity autocorrelation functions were further analyzed with eq 5 to extract the relaxation time constant of the underlying dynamics, $\tau$, which is the inverse of the relaxation rate, $\Gamma$. We note that the KWW function has been successfully employed in many dynamic investigations of colloidal dispersions and gels,[7,43−47] and is particularly useful for systems in which the particle diffusion does not follow simple Einstein−Stokes equations. Figure 6a, b, and c shows the relaxation time, $\tau$, obtained from fits of eq 5 to the USAXS−XPCS data from 10%, 15%, and 20% vol PS microspheres in glycerol suspensions as a function of $q$ for 1.0 $\mu$m PS microspheres, 1.3 $\mu$m PS microspheres, and 1.5 $\mu$m PS microspheres, respectively. In every case, in agreement with what Figure 5 shows qualitatively, we found that the relaxation time $\tau$ shows a monotonic decay as $q$ increases. This phenomenon has been observed in other colloidal dispersions in viscous media, such as magnetic colloidal particles in glycerol[5] and silica nanoparticles in 1,2 propanediol.[35] We also note that, at all $q$ values, the KWW exponent $\gamma$ was greater than 1, as shown clearly by the inset example in Figure 5 for the autocorrelation function at $q$ = 0.0002 Å$^{-1}$. This signifies that the motion of the PS microspheres is at least partially collective in nature. Interestingly, these results do not agree with those from a previous XPCS study of a similar system (PS spheres with nominal radius 665 Å in glycerol at 268 K),[4] where it was found that the intensity autocorrelation functions followed a simple exponential decay ($\gamma$ = 1) for PS suspensions with PS volume concentration as high as 28%. These results suggest that, despite the high colloidal concentration, the interparticle interaction did not disrupt the free diffusion of the particles and the PS particles still underwent Brownian-like motion. Our results suggested otherwise; at volume concentrations as low as 10%, there are partially collective motions among the PS microspheres due to their interparticle interactions. Our calculations also show that despite the relatively large size of the polystyrene spheres, the sedimentation (in our case, floatation) rate is about 2 orders of magnitude below the diffusion rate (Supporting Information), which shows that the sedimentation effects are negligible.

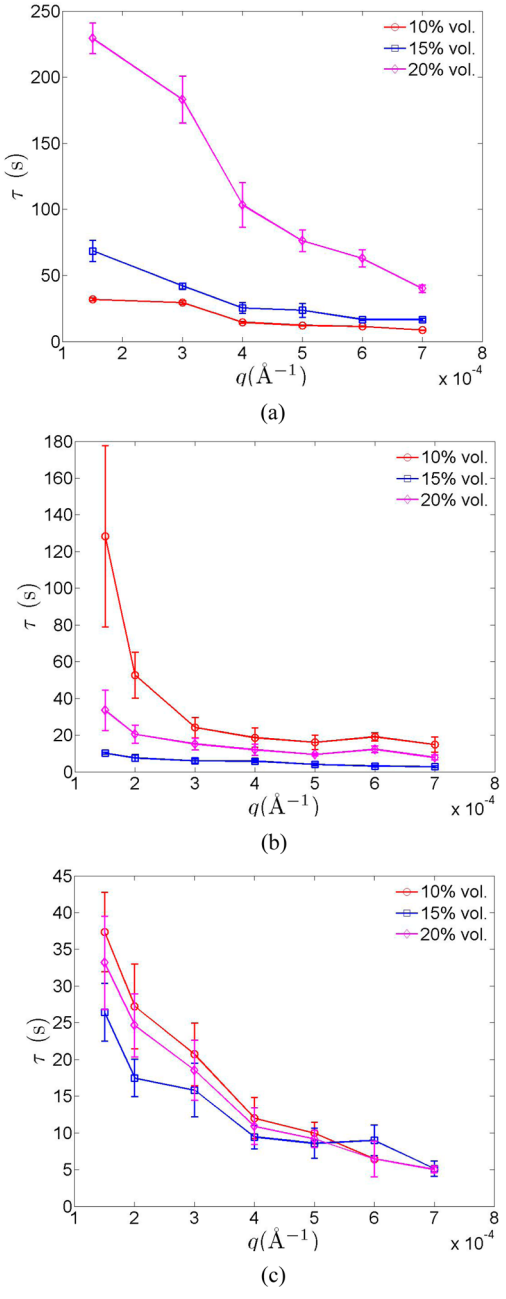


**Figure 6.** Relaxation time, $\tau$, obtained from fits of eq 5 to the USAXS−XPCS data from 10%, 15%, and 20% vol PS microspheres in glycerol suspensions as a function of $q$ for (a) 1.0 $\mu$m PS microspheres; (b) 1.3 $\mu$m PS microspheres; and (c) 1.5 $\mu$m PS microspheres.

We would also expect the dynamic time scale to be systematic with respect to PS volume fraction. As shown by Figure 6, this was not observed. For example, Figure 6a shows an increasing $\tau$ with increasing volume fraction of 1.0 $\mu$m spheres, whereas Figure 6b exhibits an apparently random $\tau$-ordering for 1.3 $\mu$m spheres. We believe that this nonsystematic behavior is due to the small amount of remnant water in the solvent; the transfer of microspheres from original aqueous suspension to glycerol is not completed with a vacuum desiccation procedure because water and glycerol are well mixed.[48] The viscosity of water−glycerol mixtures strongly depends on the amount of water when the glycerol/water ratio is high. For example, at 10 °C, a 99:1 glycerol to water mass-ratio solution has a viscosity of 3090 mPa s.[49] At the same temperature, a 96:4 solution has a viscosity of just 1580 mPa s. Therefore, a small change in the amount of water in the suspension can lead to a drastic change in the effective viscosity of the solvent, thus changing the time scale of the associated PS microsphere dynamics.

Analogous to the case of dilute suspensions, the relaxation rate of a concentrated suspension with collective motion can be described by $\Gamma = q^2D(q)$, where $D(q)$ is a wave-vector dependent, effective diffusion constant that describes the collective diffusion of interacting particles.[5,50] The ratio between $D_0$ and $D(q)$, where $D_0$ is the diffusion constant for a single particle undergoing Brownian motion in the same medium under the same conditions, therefore, is proportional to $q^2\tau$, given that $\tau = \Gamma^{-1}$. Figure 7 shows an example of the $q^2\tau$ dependency on $q$. For each of the different samples, we found that the inverse of the effective diffusion coefficients displays a peak that mimics the peaks in the static structure factors. Here, the equilibrium structure of the suspension is represented by the static structure factor, which shows the configuration of the


dx.doi.org/10.1021/la3044768 | Langmuir 2013, 29, 1379−1387

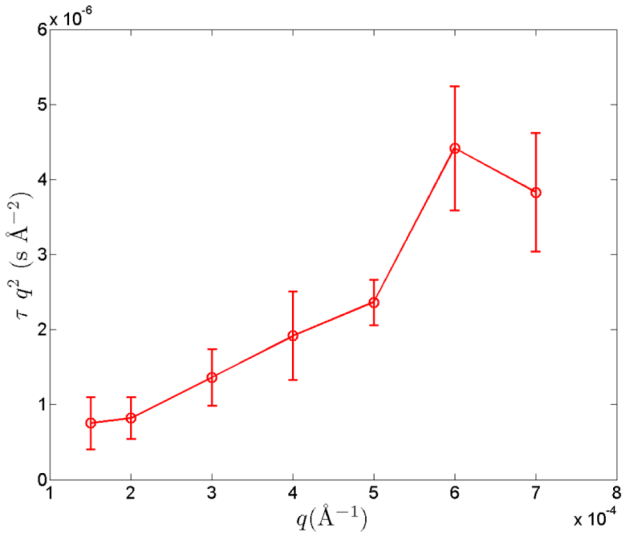


**Figure 7.** An example of un-normalized $D_0/D(q)$ for 1.3 $\mu$m, 20% vol PS microspheres in glycerol suspensions.

low free energy state in the reciprocal space. The effective diffusion constant, on the other hand, quantifies the speed of particle motion in these concentrated suspensions. This proportionality suggests that the lowest free-energy configuration in the static case also has a long lifetime, as illustrated by the peak in the inverse of the effective diffusion coefficient.[51,52] The proportionality between the structure factor and $q^2\tau$, suggestive of de Gennes narrowing[53] at interparticle length scales, also indicates that the slow, local dynamics follows a simple alpha relaxation mode, a distinct feature of the collective diffusion in local structural rearrangements.

Finally, we examined the power-law behavior of the $q$-dependent time scales. This is demonstrated in Figure 8 where the logarithm of $\tau$ is plotted as a function of the logarithm of $q$. Our results show that, in all cases, the logarithm of $\tau$ is approximately linearly related to the logarithm of $q$, with the slope being $-1.06 \pm 0.22$, that is, $\tau \approx q^{-1.06\pm0.22}$. This inverse $\tau \approx q^{-1}$ relationship was also observed in various dynamic processes ranging from nanoparticle suspensions to depletion gels.[10,35,45,54,55] Theoretically, this behavior was explained by Cipellettie et al.[56] for the case where the underlying dynamics can be described by particle motions due to relaxation of the heterogeneous local stress. As a result of this mechanism, a collective motion of the particles and their neighboring particles again emerges.[47,56]

## CONCLUDING REMARKS

In this Article, we have presented the first systematic study of equilibrium dynamics with USAXS−XPCS, a dynamic approach capable of filling the gap between DLS and conventional XPCS in the time/frequency−scattering vector/length scale domains. Taking advantage of the Bonse−Hart type crystal optics, USAXS−XPCS provides access to a $q$ range that corresponds to large structures (~0.1−1 $\mu$m) whose dynamics are inherently slow.

With USAXS and USAXS−XPCS, we probed the static and dynamic behaviors of concentrated suspensions of a series of different sized polystyrene microspheres dispersed in glycerol for volume concentrations between 10% and 20%. These samples, although fundamentally very simple, present a challenge for characterization with light-scattering techniques due to their optical opaqueness originating from multiple scattering. Hard X-rays, on the other hand, have much smaller

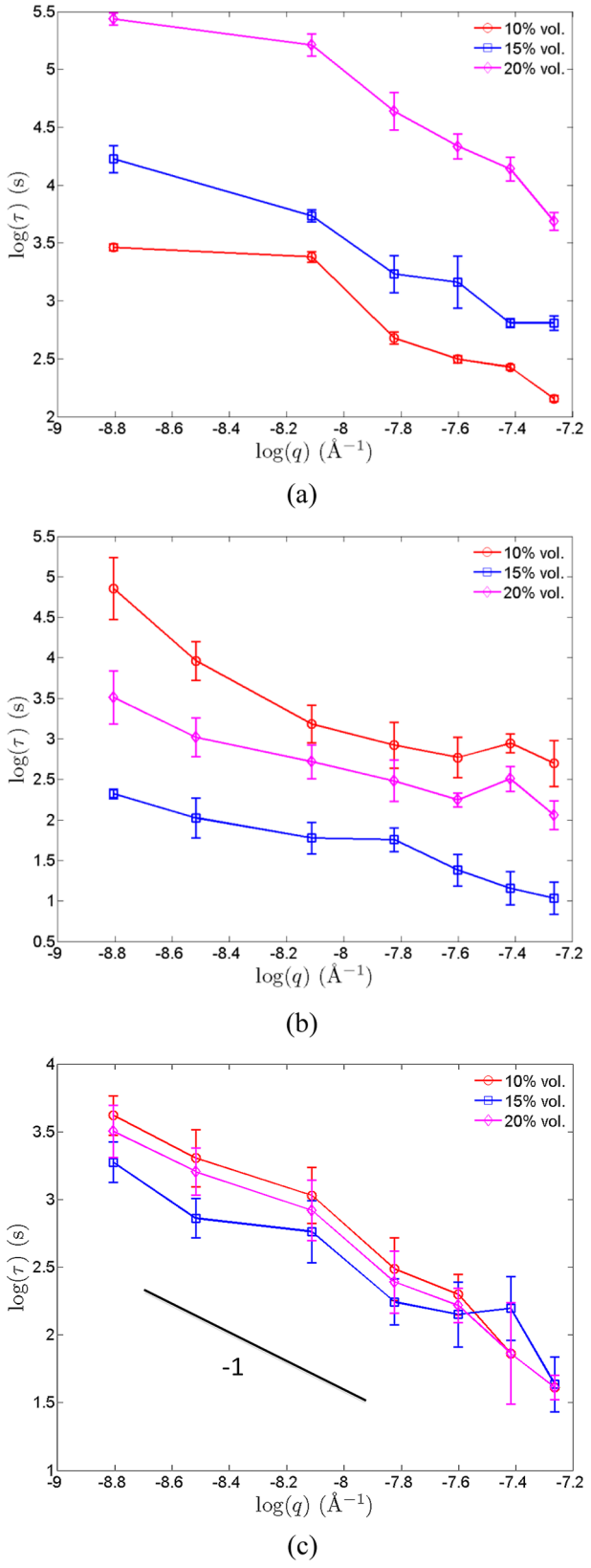


**Figure 8.** Scaling behavior of dynamic time scale as a function of $q$: (a) 1.0 $\mu$m, (b) 1.3 $\mu$m, and (c) 1.5 $\mu$m microspheres in glycerol. [All uncertainties in this Article represent one standard deviation.]


dx.doi.org/10.1021/la3044768 | Langmuir 2013, 29, 1379−1387

scattering cross sections and are not hindered by multiple scattering.

The USAXS measurements proved that these PS spheres are highly monodisperse in size, which make them good model systems for the investigation of particle dynamics in concentrated suspensions. The structure factors of these suspensions can be satisfactorily modeled with Percus−Yevick hard sphere potentials, a behavior resembling that previously identified in a PS nanocolloid suspension in glycerol, despite the apparent size difference.

An analysis of the USAXS−XPCS data of these suspensions shows that their intensity autocorrelation functions are best described by the Kohlrausch−Williams−Watts function, which suggests that these microspheres undergo a collective motion, instead of simple Brownian motion found for the PS nanocolloids in glycerol in the relevant concentration range. The inverse of the effective diffusion coefficients displays a peak when plotting against $q$. This peak is similar to the primary peak in the static structure factor. The proportionality between these two peaks, a characteristic of de Gennes narrowing, suggests that these particles undergo collective motion. Furthermore, we found that the relaxation time is inversely proportional to the scattering vector, a behavior also related to collective motion of particles.

Although the $q$ range covered by USAXS−XPCS is small, its relevant size range, however, is important to many material systems, in particular soft materials such as various polymer solutions and blends, organic and biological micelles, and colloidal dispersions. It is also our hope that this first systematic USAXS−XPCS study of simple colloidal systems serves as an example to demonstrate the capability of USAXS−XPCS as a new dynamic technique, a technique that can help in the understanding of the vastly unexplored yet critically important field of material dynamics.

## ■ ASSOCIATED CONTENT

### Supporting Information

Additional experimental details. This material is available free of charge via the Internet at http://pubs.acs.org.

## ■ AUTHOR INFORMATION


### Corresponding Author

*E-mail: fan.zhang@nist.gov.


### Notes

The authors declare no competing financial interest.

## ■ ACKNOWLEDGMENTS

We thank Larry Lurio for his comments and discussions. ChemMatCARS Sector 15 is principally supported by the National Science Foundation/Department of Energy under grant number NSF/CHE-0822838. Use of the Advanced Photon Source was supported by the U.S. Department of Energy, Office of Science, Office of Basic Energy Sciences, under contract no. DE-AC02-06CH11357.

## ■ REFERENCES


(1) Berne, B. J.; Pecora, R. *Dynamic Light Scattering: With Applications to Chemistry, Biology, and Physics*; Dover Publications, Inc.: Mineola, NY, 2000.

(2) ThurnAlbrecht, T.; Steffen, W.; Patkowski, A.; Meier, G.; Fischer, E. W.; Grubel, G.; Abernathy, D. L. Photon correlation spectroscopy of colloidal palladium using a coherent x-ray beam. *Phys. Rev. Lett.* **1996**, *77*, 5437−5440.

(3) Lurio, L. B.; Lumma, D.; Sandy, A. R.; Borthwick, M. A.; Falus, P.; Mochrie, S. G. J.; Pelletier, J. F.; Sutton, M.; Regan, L.; Malik, A.; Stephenson, G. B. Absence of scaling for the intermediate scattering function of a hard-sphere suspension: Static and dynamic x-ray scattering from concentrated polystyrene latex spheres. *Phys. Rev. Lett.* **2000**, *84*, 785−788.

(4) Lumma, D.; Lurio, L. B.; Borthwick, M. A.; Falus, P.; Mochrie, S. G. J. Structure and dynamics of concentrated dispersions of polystyrene latex spheres in glycerol: Static and dynamic x-ray scattering. *Phys. Rev. E* **2000**, *62*, 8258−8269.

(5) Lal, J.; Abernathy, D.; Auvray, L.; Diat, O.; Grubel, G. Dynamics and correlations in magnetic colloidal systems studied by X-ray photon correlation spectroscopy. *Eur. Phys. J. E* **2001**, *4*, 263−271.

(6) Banchio, A. J.; Gapinski, J.; Patkowski, A.; Haussler, W.; Fluerasu, A.; Sacanna, S.; Holmqvist, P.; Meier, G.; Lettinga, M. P.; Nagele, G. Many-body hydrodynamic interactions in charge-stabilized suspensions. *Phys. Rev. Lett.* **2006**, *96*, 138303.

(7) Fluerasu, A.; Moussaid, A.; Madsen, A.; Schofield, A. Slow dynamics and aging in colloidal gels studied by x-ray photon correlation spectroscopy. *Phys. Rev. E* **2007**, *76*, 010401.

(8) Guo, H. Y.; Bourret, G.; Corbierre, M. K.; Rucareanu, S.; Lennox, R. B.; Laaziri, K.; Piche, L.; Sutton, M.; Harden, J. L.; Leheny, R. L. Nanoparticle motion within glassy polymer melts. *Phys. Rev. Lett.* **2009**, *102*, 075702.

(9) Falus, P.; Borthwick, M. A.; Mochrie, S. G. J. Fluctuation dynamics of block copolymer vesicles. *Phys. Rev. Lett.* **2005**, *94*, 016105.

(10) Chung, B.; Ramakrishnan, S.; Bandyopadhyay, R.; Liang, D.; Zukoski, C. F.; Harden, J. L.; Leheny, R. L. Microscopic dynamics of recovery in sheared depletion gels. *Phys. Rev. Lett.* **2006**, *96*, 228301.

(11) Falus, P.; Narayanan, S.; Sandy, A. R.; Mochrie, S. G. J. Crossover from stretched to compressed exponential relaxations in a polymer-based sponge phase. *Phys. Rev. Lett.* **2006**, *97*, 066102.

(12) Patel, A. J.; Narayanan, S.; Sandy, A.; Mochrie, S. G. J.; Garetz, B. A.; Watanabe, H.; Balsara, N. P. Relationship between structural and stress relaxation in a block-copolymer melt. *Phys. Rev. Lett.* **2006**, *96*, 257801.

(13) Gutt, C.; Ghaderi, T.; Chamard, V.; Madsen, A.; Seydel, T.; Tolan, M.; Sprung, M.; Grubel, G.; Sinha, S. K. Observation of heterodyne mixing in surface x-ray photon correlation spectroscopy experiments. *Phys. Rev. Lett.* **2003**, *91*, 076104.

(14) Kim, H.; Ruhm, A.; Lurio, L. B.; Basu, J. K.; Lal, J.; Lumma, D.; Mochrie, S. G. J.; Sinha, S. K. Surface dynamics of polymer films. *Phys. Rev. Lett.* **2003**, *90*, 068302.

(15) Madsen, A.; Seydel, T.; Sprung, M.; Gutt, C.; Tolan, M.; Grubel, G. Capillary waves at the transition from propagating to overdamped behavior. *Phys. Rev. Lett.* **2004**, *92*, 096104.

(16) Jiang, Z.; Mukhopadhyay, M. K.; Song, S.; Narayanan, S.; Lurio, L. B.; Kim, H.; Sinha, S. K. Entanglement effects in capillary waves on liquid polymer films. *Phys. Rev. Lett.* **2008**, *101*, 246104.

(17) Sutton, M.; Mochrie, S. G. J.; Greytak, T.; Nagler, S. E.; Berman, L. E.; Held, G. A.; Stephenson, G. B. Observation of speckle by diffraction with coherent X-rays. *Nature* **1991**, *352*, 608−610.

(18) Brauer, S.; Stephenson, G. B.; Sutton, M.; Bruning, R.; Dufresne, E.; Mochrie, S. G. J.; Grubel, G.; Alsnielsen, J.; Abernathy, D. L. X-ray-intensity fluctuation spectroscopy observations of critical-dynamics in Fe3al. *Phys. Rev. Lett.* **1995**, *74*, 2010−2013.

(19) Dierker, S. B.; Pindak, R.; Fleming, R. M.; Robinson, I. K.; Berman, L. X-Ray photon-correlation spectroscopy study of Brownian-motion of gold colloids in glycerol. *Phys. Rev. Lett.* **1995**, *75*, 449−452.

(20) Grubel, G.; Abernathy, D. L. Diffraction and correlation spectroscopy with coherent x-rays. In *Coherent Electron-Beam X-Ray Sources: Techniques and Applications*; Freund, A. K., Freund, H. P., Howells, M. R., Eds.; SPIE: CA, 1997; pp 103−109.

(21) Zhang, F.; Ilavsky, J. Ultra-small-angle X-ray scattering of polymers. *Polym. Rev.* **2010**, *50*, 59−90.

(22) Narayanan, T. High brilliance small-angle X-ray scattering applied to soft matter. *Curr. Opin. Colloid Interface Sci.* **2009**, *14*, 409−415.

(23) Cerbino, R.; Trappe, V. Differential dynamic microscopy: Probing wave vector dependent dynamics with a microscope. *Phys. Rev. Lett.* **2008**, *100*, 188102.
(24) Wilson, L. G.; Martinez, V. A.; Schwarz-Linek, J.; Tailleur, J.; Bryant, G.; Pusey, P. N.; Poon, W. C. K. Differential dynamic microscopy of bacterial motility. *Phys. Rev. Lett.* **2011**, *106*, 018101.
(25) Giavazzi, F.; Brogioli, D.; Trappe, V.; Bellini, T.; Cerbino, R. Scattering information obtained by optical microscopy: Differential dynamic microscopy and beyond. *Phys. Rev. E* **2009**, *80*, 031403.
(26) Lu, P. J.; Giavazzi, F.; Angelini, T. E.; Zaccarelli, E.; Jargstorff, F.; Schofield, A. B.; Wilking, J. N.; Romanowsky, M. B.; Weitz, D. A.; Cerbino, R. Characterizing concentrated, multiply scattering, and actively driven fluorescent systems with confocal differential dynamic microscopy. *Phys. Rev. Lett.* **2012**, *108*, 218103.
(27) Cerbino, R.; Peverini, L.; Potenza, M. A. C.; Robert, A.; Bosecke, P.; Giglio, M. X-ray-scattering information obtained from near-field speckle. *Nat. Phys.* **2008**, *4*, 238−243.
(28) Lu, X. H.; Mochrie, S. G. J.; Narayanan, S.; Sandy, A. R.; Sprung, M. X-ray near-field speckle: implementation and critical analysis. *J. Synchrotron Radiat.* **2011**, *18*, 823−834.
(29) Zhang, F.; Allen, A. J.; Levine, L. E.; Ilavsky, J.; Long, G. G.; Sandy, A. R. Development of ultra-small-angle X-ray scattering - X-ray photon correlation spectroscopy. *J. Appl. Crystallogr.* **2011**, *44*, 200−212.
(30) Zhang, F.; Allen, A. J.; Levine, L. E.; Ilavsky, J.; Long, G. G. Ultra-small-angle X-ray scattering-X-ray photon correlation spectroscopy: A new measurement technique for in-situ studies of equilibrium and nonequilibrium dynamics. *Metall. Mater. Trans. A* **2012**, *43A*, 1445−1453.
(31) Ilavsky, J.; Jemian, P. R.; Allen, A. J.; Zhang, F.; Levine, L. E.; Long, G. G. Ultra-small-angle X-ray scattering at the Advanced Photon Source. *J. Appl. Crystallogr.* **2009**, *42*, 469−479.
(32) Ilavsky, J.; Jemian, P. R. Irena: tool suite for modeling and analysis of small-angle scattering. *J. Appl. Crystallogr.* **2009**, *42*, 347−353.
(33) Lake, J. A. An iterative method of slit-correcting small-angle X-ray data. *Acta Crystallogr.* **1967**, *23*, 191−194.
(34) Grubel, G.; Zontone, F. Correlation spectroscopy with coherent X-rays. *J. Alloys Compd.* **2004**, *362*, 3−11.
(35) Caronna, C.; Chushkin, Y.; Madsen, A.; Cupane, A. Dynamics of nanoparticles in a supercooled liquid. *Phys. Rev. Lett.* **2008**, *100*, 055702.
(36) Pusey, P. N. *Liquids, Freezing and the Glass Transition*; North-Holland: Amsterdam, 1991.
(37) Kao, M. H.; Yodh, A. G.; Pine, D. J. Observation of Brownian motion on the time scale of hydrodynamic interactions. *Phys. Rev. Lett.* **1993**, *70*, 242−245.
(38) Mason, T. G.; Weitz, D. A. Linear viscoelasticity of colloidal hard sphere suspensions near the glass transition. *Phys. Rev. Lett.* **1995**, *75*, 2770−2773.
(39) Rutgers, M. A.; Dunsmuir, J. H.; Xue, J. Z.; Russel, W. B.; Chaikin, P. M. Measurement of the hard-sphere equation of state using screened charged polystyrene colloids. *Phys. Rev. B* **1996**, *53*, 5043−5046.
(40) Hayter, J. B.; Penfold, J. An analytic structure factor for macroion solutions. *Mol. Phys.* **1981**, *42*, 109−118.
(41) Kotlarchyk, M.; Chen, S. H. Analysis of small-angle neutron-scattering spectra from polydisperse interacting colloids. *J. Chem. Phys.* **1983**, *79*, 2461−2469.
(42) Gutt, C.; Ghaderi, T.; Tolan, M.; Sinha, S. K.; Grubel, G. Effects of partial coherence on correlation functions measured by x-ray photon correlation spectroscopy. *Phys. Rev. B* **2008**, *77*, 094133.
(43) Pontoni, D.; Narayanan, T.; Petit, J. M.; Grubel, G.; Beysens, D. Microstructure and dynamics near an attractive colloidal glass transition. *Phys. Rev. Lett.* **2003**, *90*, 188301.
(44) Duri, A.; Autenrieth, T.; Stadler, L. M.; Leupold, O.; Chushkin, Y.; Grubel, G.; Gutt, C. Two-dimensional heterogeneous dynamics at the surface of a colloidal suspension. *Phys. Rev. Lett.* **2009**, *102*, 145701.
(45) Bandyopadhyay, R.; Liang, D.; Yardimci, H.; Sessoms, D. A.; Borthwick, M. A.; Mochrie, S. G. J.; Harden, J. L.; Leheny, R. L. Evolution of particle-scale dynamics in an aging clay suspension. *Phys. Rev. Lett.* **2004**, *93*, 228302.
(46) Bellour, M.; Knaebel, A.; Harden, J. L.; Lequeux, F.; Munch, J. P. Aging processes and scale dependence in soft glassy colloidal suspensions. *Phys. Rev. E* **2003**, *67*, 031405.
(47) Cipelletti, L.; Ramos, L. Slow dynamics in glassy soft matter. *J. Phys.: Condens. Matter* **2005**, *17*, R253−R285.
(48) Cristancho, D. M.; Delgado, D. R.; Martínez, F.; Fakhree, M. A. A.; Jouyban, A. Volumetric properties of glycerol + water mixtures at several temperatures and correlation with the Jouyban-Acree model. *Rev. Colomb. Cienc. Quim.-Farm.* **2011**, *40*, 92−115.
(49) Dorsey, N. E. *Properties of Ordinary Water-Substance*; Reinhold: New York, 1940.
(50) Gapinski, J.; Patkowski, A.; Banchio, A. J.; Buitenhuis, J.; Holmqvist, P.; Lettinga, M. P.; Meier, G.; Nagele, G. Structure and short-time dynamics in suspensions of charged silica spheres in the entire fluid regime. *J. Chem. Phys.* **2009**, *130*, 084503.
(51) Philipse, A. P.; Vrij, A. Determination of static and dynamic interactions between monodisperse, charged silica spheres in an optically matching, organic-solvent. *J. Chem. Phys.* **1988**, *88*, 6459−6470.
(52) Phalakornkul, J. K.; Gast, A. P.; Pecora, R.; Nagele, G.; Ferrante, A.; Mandl-Steininger, B.; Klein, R. Structure and short-time dynamics of polydisperse charge-stabilized suspensions. *Phys. Rev. E* **1996**, *54*, 661−675.
(53) Segre, P. N.; Pusey, P. N. Scaling of the dynamic scattering function of concentrated colloidal suspensions. *Phys. Rev. Lett.* **1996**, *77*, 771−774.
(54) Roshi, A.; Barjami, S.; Iannacchione, G. S.; Paterson, D.; McNulty, I. Structure and dynamics of a nanocolloidal silica gel dispersion. *Phys. Rev. E* **2006**, *74*, 31913.
(55) Srivastava, S.; Kandar, A. K.; Basu, J. K.; Mukhopadhyay, M. K.; Lurio, L. B.; Narayanan, S.; Sinha, S. K. Complex dynamics in polymer nanocomposites. *Phys. Rev. E* **2009**, *79*, 041603.
(56) Cipelletti, L.; Ramos, L.; Manley, S.; Pitard, E.; Weitz, D. A.; Pashkovski, E. E.; Johansson, M. Universal non-diffusive slow dynamics in aging soft matter. *Faraday Discuss.* **2003**, *123*, 237−251.